Al-Nahrain Journal for Engineering Sciences **NJES** 25(1)06-11, 2022
http://doi.org/10.29194/NJES.25010006

Single Bubble Breakage in Oil Under Stirring Conditions

Basim O. Hasan

Authors affiliations:
1) Dept. of Chemical Eng., Al-Nahrain University, Iraq.
basimohasan13@gmail.com,
basimhasan2017@eng.nahrainuniv.edu.iq

Paper History:

Received: 10th Aug. 2021

Revised: 12th Jan. 2022

Accepted: 22nd Feb. 2022

Abstract

An experimental study on single bubble breakage in the stirred tank in oil as a continuous phase was carried out for a range of stirring speeds (220 to 430 rpm). The results are compared with bubble breakage in water that was conducted by Hasan et al. (2021) to investigate the effect of physical properties of the continuous phase on the breakage rate. The breakage events in the impeller were captured and analyzed using a high speed camera. It was found that the breakage rate represented by breakage probability and the number of produced daughter bubbles (fragments) are directly proportional to the stirring speed. The breakage probability and the number of produced daughter bubbles in oil were noticeably lower than that in water indicating the role the continuous phase viscosity plays in reducing the breakage rate.

Keywords: Bubble Breakage; Stirred Tank; Stirring Speed; Breakage Rate; Oil.

1. Introduction

Gas-liquid and liquid-liquid dispersions are of industrial significance as such systems are encountered in the various production processes in the chemical and petrochemical industries, food processing, bioreactors, etc. Bubble and drop (fluid particle) play an important role in mass, heat, and momentum transfer in industrial processes. The dispersion of gas in liquids has practical importance due to its role in determining the interfacial area [1-3].

In stirred tank systems (such as biochemical reactors and mixing operations), the fluid particle behavior is complicated due to the effect of hydrodynamics and different local values of turbulence energy. In the stirred tank there are regions of high turbulence intensity that rive the bubble to be impeller region which increases the BP and the produced fragments. [4].

The dynamics behavior of the bubble is largely influenced by operating parameters such as flow velocity, viscosity and stirring time [5-8]. Several authors [9-11] reported a decrease in breakage rate with increasing continuous phase viscosity. While [12] found that the effect of continuous phase viscosity on the breakage rate is a function of the stirring speed.

The bubble breakage rate in a turbulent field is calculated as [1]:

$$B(d_p) = \frac{1}{t_b}\frac{n}{n_T} \qquad (1)$$

Where B is the breakage rate which is dependent on bubble diameter (d_p) n is the number of breakages, t_b is the breakage time, and n_T is the number of bubbles released in the field which are termed "mother bubbles". The BP is the ratio between the number of breakages and the total number of bubbles injected into the field. Therefore, the BP is determined by counting the number of breakages by visual observation via a high camera.

The current work aims to study the breakage rate of air bubbles in the oil continuous phase for a range of power input and compare the results with that in the water continuous phase reported by [14]. This is for gaining a deeper insight into the influence of physical properties of the continuous phase on the breakage rate.

2. Experimental setup

A schematic diagram of the experimental setup is shown in Figure 1. The rig has been described in detail in previous work [15]. The investigated stirring rates were 220, 300, 380, and 430 rpm. The values of energy dissipation was calculated using[16-17]:

$$\varepsilon = \frac{N_p D_i^5}{V_l} \qquad (2)$$

where V_l is the volume of the liquid (m^3) in the tank, N is the stirring speed (rps), N_p is the power number, and Di is the impeller diameter in m. It was reported that Np = 5.5 for the Rushton turbine [16]. For V_l= 6 liters (0.006 m^3), the values of energy dissipation rates corresponding to the stirring rate that was considered in this work are 0.08, 0.21, 0.42, and 0.61 m^2/s^3 respectively.

Each experiment was included at least 500 breakage tests. The average mother bubble diameter when it was still spherical before deformation was found to be 4.5±0.15 mm. Bubble breakage behavior

was imaged by a high speed camera. The experiments were carried out in, the light oil continuous phase and compared with the work of [14] that used the water continuous phase. This was to study the effect of viscosity on bubble breakage behavior. Light engine oil with a viscosity = 0.570 kg/m.s and density = 885 kg/m^3 at 25 ^{o}C[18] was used. The experiments were carried out at a room temperature of 20±1 ^{o}C. The BP was calculated a:

$$BP\ \% = \frac{n}{n_T} \times 100 \qquad (3)$$

Where n is the number of broken mother bubbles (or a number of breakages) for a total number of injected bubbles (n_T). The average number of daughter bubbles (fragments) was calculated as:

$$n_a = \frac{n_d}{n} \qquad (4)$$

Where n_a is the average number of fragments (or daughter bubbles) and n_d is the summation of the number of fragments produced from n broken mother bubbles (or n breakages) at a specific power input.

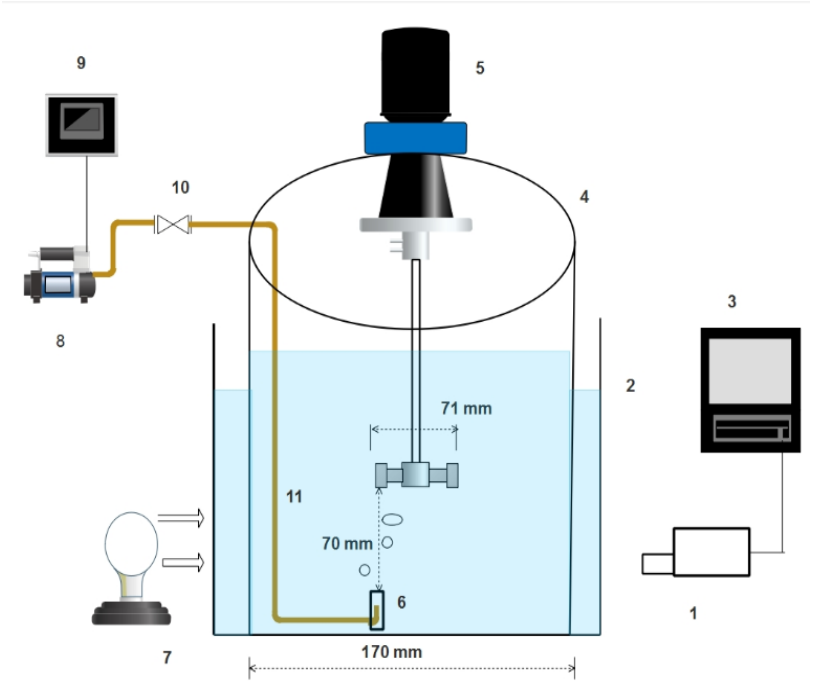

Figure 1: Experimental rig: 1. High-speed camera, 2. outside tank 3. computer, 4. Inside the cylindrical tank, 5. stirrer, 6. glass tube, 7. projector, 8. Air pump, 9. on-off controller, 10. control valve[15].

3. Results and Discussion

3.1 Breakage events

A high speed camera was used to identify breakage events in oil as a continuous phase, showing that the breakage dynamics occurred after a high degree of deformation which depended on the agitation speed. In general, the number of breakages (or breakage probability) and a number of fragments (daughter bubbles) are clearly less than in water. Figure 2a shows different deformed shapes the bubble exhibits when traveling in oil continuous phase under turbulent flow conditions. Necking (a), elongation (b), and flattening (c and d) are seen

Fig. 2b shows a series of images of mother bubble breakages at different stirring speeds at which the bubble breaks up in oil at the injection location after different degrees of deformation. Case **a** is a binary breakage at 220 rpm in which necking is formed and becomes thinner until the break up which produces two unequal-sized daughter bubbles. Case **b** shows ternary breakage at 300 rpm after the occurrence of necking to form one large daughter bubble and two smaller ones. Case **c** is a ternary breakage at 380 rpm in which the mother bubble breaks up to form two large daughter bubbles with one small. In these cases, the mother bubble is starched by flow currents acting on the injection position and pushed into the right which results in a breakup that produces unequal-sized daughter bubbles.

3.2 Overall Breakage probability (BP)

It was demonstrated that the impeller region is characterized by turbulence levels [19-21]. Close to the impeller, the bubble undergoes a high scale of deformation. Besides, the BP is high, and the number of generated daughter bubbles is high. In addition, for high stirring speed, the bubbles follow the irregular trajectory.

Investigations concerning the hydrodynamics in the stirred tank [19-21] revealed that the level of energy dissipated close to the impeller high compared to other tank locations. The high energy level at the impeller blades causes a high breakage rate due to the high-velocity fluctuations which are about half the blade's speed[21,22]. Several studies[23-25] ejected flow current close to the blade's shear layer around the blade plays an important role in the breakage events. Away from the blade, the main reason for the breakage is the velocity fluctuation.

The boundary layer in the vicinity of the wall is responsible for deforming and breaking the drop/bubble even though the rotation speed is low.

[23] stated that the flow currents in the front of the blade lead to breaking the drops/bubbles by stretching them. This behavior is also observed in the present work. According to [23], the flow pattern in front of the blade breaks the fluid particles by stretching them; which is in accordance with the present observation [9,26] postulated that there are strong shearing forces in the boundary layer of the blades, which is responsible for the occurrence of breakage.

Figure 3 shows the overall breakage probability (PB) in both continuous phases of water[15] and oil, versus stirring speed. It is clear that the PB increases with increasing stirring speed. The BP in oil is lower than in water. Fig. 4 presents the probability of multiple breakages versus stirring speed. At low speed (220 rpm) the probability of multiple breakages is 80% for water and 76.3% for oil. This percentage increases with increasing speed to become 100% at high speeds for both continuous phases, i.e no binary breakage close to the impeller.

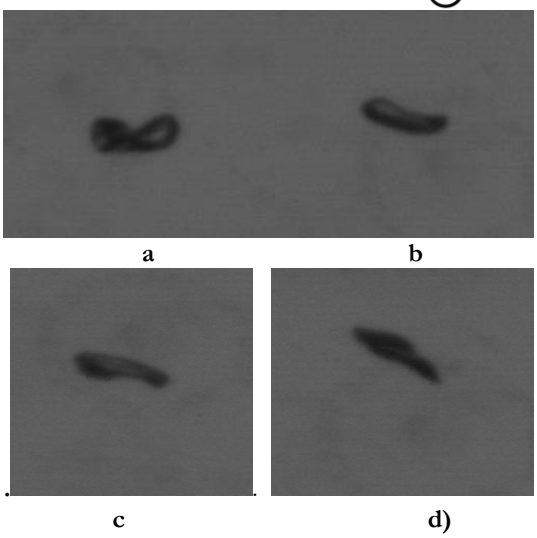

Figure 2a: different deformed shapes of the bubble during traveling in turbulent flow of oil, a) necking, b) elongation, c) flattening, N=300 rpm

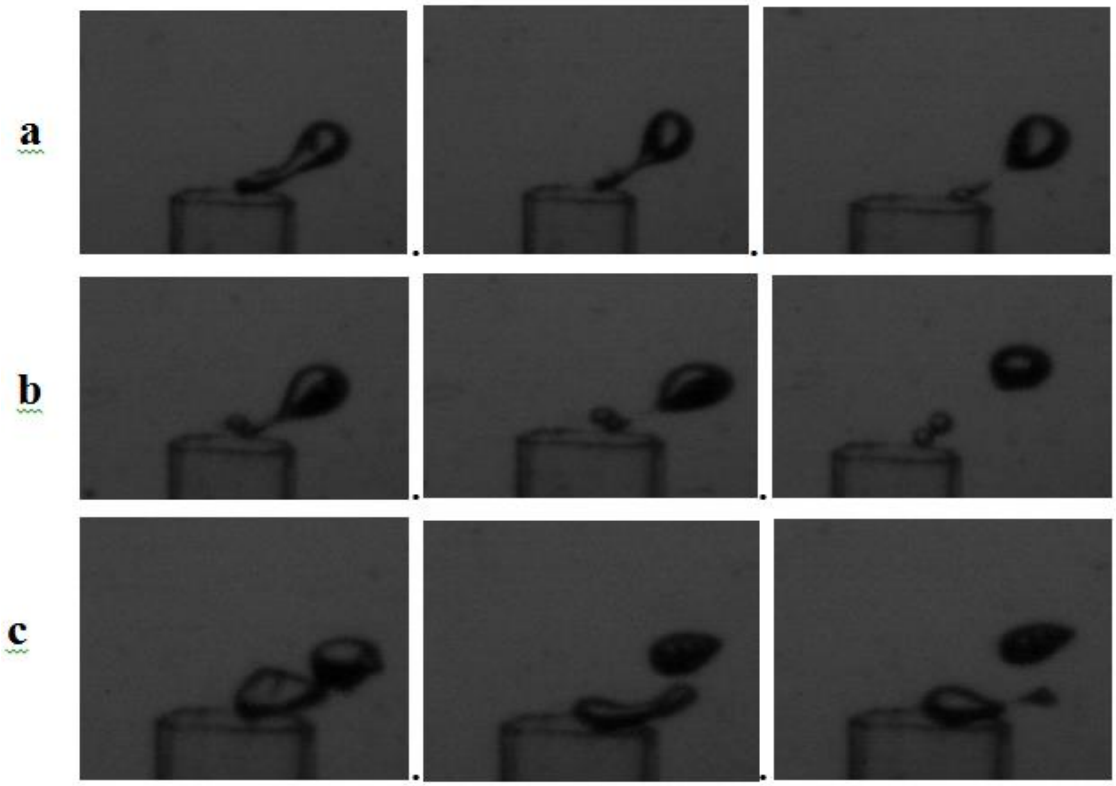

Figure 2b: Breakage of mother bubbles in oil after necking at a) N=220 rpm, b) N=300 rpm, c) N=380 rpm.

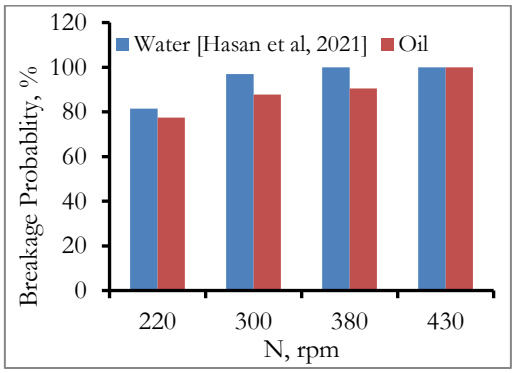

Figure 3: Overall breakage probability versus stirring speed for water and oil continuous phases.

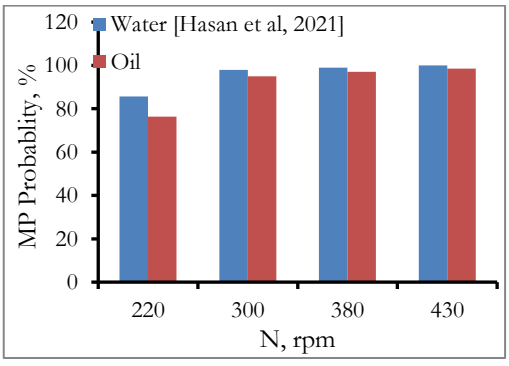

Figure 4: Multiple breakage probability vs. stirring speed.

3.3 Number of daughter bubbles (fragments)

Figure 5a presents images taken by a high speed camera close to the impeller indicating the formation of a different number of daughter bubbles for different speeds. The average number of daughter bubbles (fragments) per breakage in oil is presented in Fig. 5b as compared with water [14]. It can be seen that for the lowest agitation speed (220 rpm) the average number of daughter bubbles in both phases is 4, while for 300 rpm the number is 7.3 in water and 6.8 in oil, for 380 rpm it is 8.8 in water, and 8 in oil, and for 430 rpm it is 12.4 in water and 9.2 in oil.

Figures 6a to 6d show the number distribution of fragments (daughter bubbles) in region C versus stirring speed for both continuous phases. Fig. 16a is for the lowest stirring speed and shows that the produced number of fragments is between 2 and 8 for both phases. In this case, breakages in oil result in a higher percentage of 2 to 3 fragments while breakages in water result in a higher percentage of 4 to 8 fragments. Fig. 16b for 300 rpm indicates a little probability of 12 to 13 fragments for both phases. It can also be seen from Fig. 16b that there are no binary or ternary breakages in water (zero percentage) and in oil the percentage of such breakages are small. In this case (300 rpm) the highest probability is for 7-8 fragments in both phases. With increasing stirring speed to 380 (Fig. 16c), the percentage of 2 to 4 fragments in water is zero while there is a low probability (5-10%) for oil. At the other end of the scale, there are up to 17 fragments produced in water and up to 15 in oil. In this case, the highest probability is for 9-11 fragments in both phases. For a stirring speed of 430 rpm, Fig. 16d shows that the number of fragments is 20 in water and 17 in oil. There is also a noticeable decrease in the probability of breakages producing a low number of fragments, especially in water. In this case, the probability is highest for the production of 12 to 17 fragments in water and 7 to 11 in oil. The breakage probability and the number of daughter bubbles in oil are lower than in water. This is due to the lower breakage rate of bubbles in oil than in water.

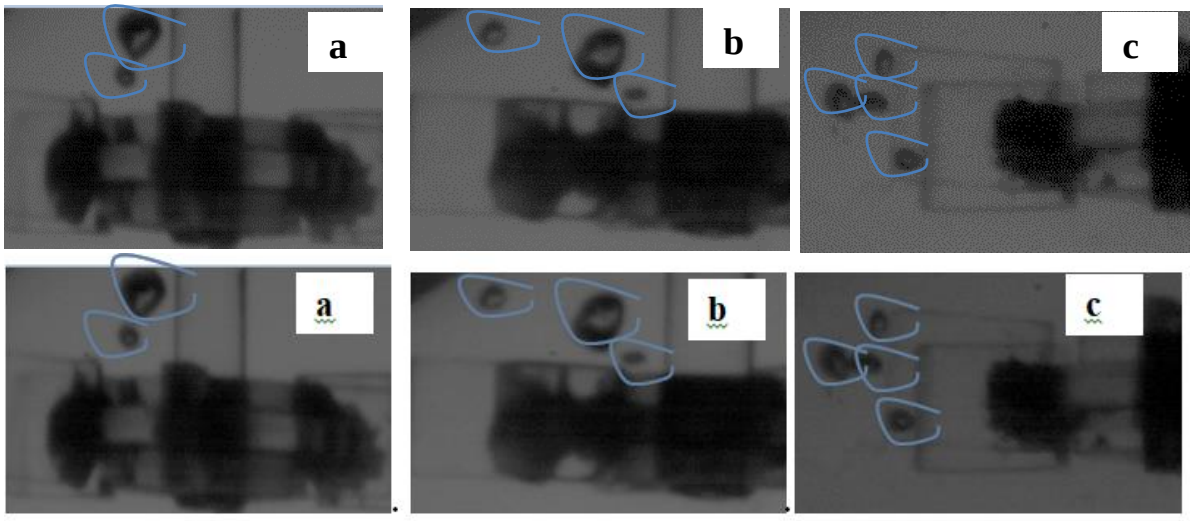

Figure 5a: Fragmentation of mother bubble to different number daughter bubbles close to the impeller, a) two daughter bubbles, N=220 rpm b) 3 daughter bubbles, N= 300 rpm c) 4 daughter bubbles, N= 380 rpm.

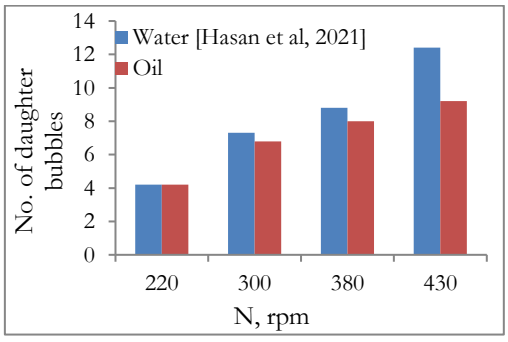

Figure 5b: Average number of daughter bubbles vs. stirring speed.

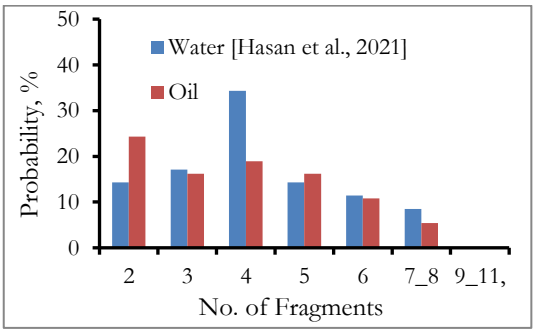

Figure 6a: Number distribution of fragments in region A at a stirring speed of 220 rpm.

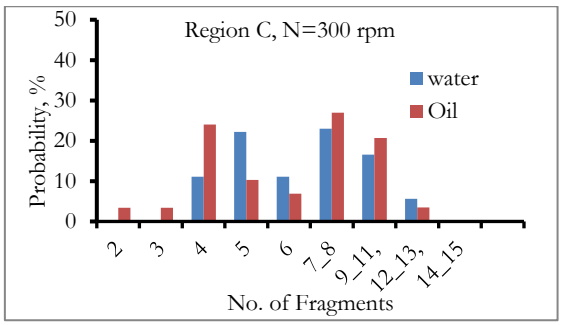

Figure 6b: Number distribution of fragments in region A at a stirring speed of 300 rpm.

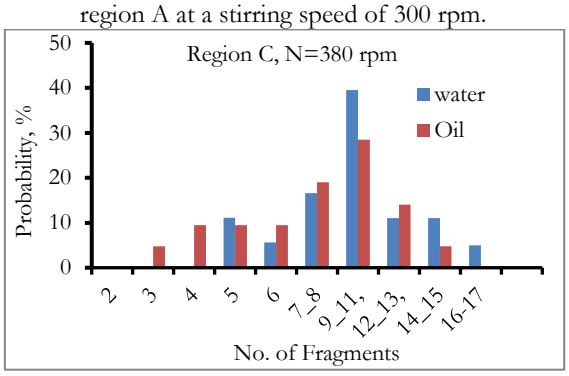

Figure 6c: Number distribution of fragments in region A at a stirring speed of 380 rpm.

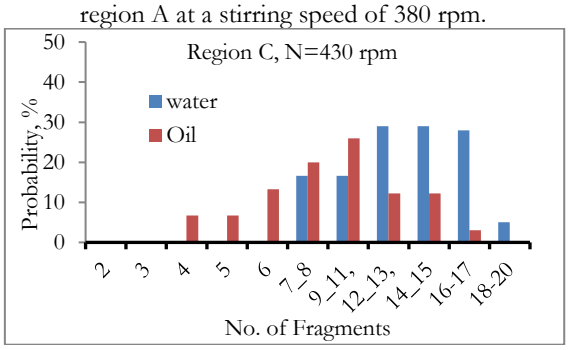

Figure 6d: Number distribution of fragments in region A at a stirring speed of 430 rpm.

Fig. 7 shows a comparison between the effects of agitation speeds on the number of produced daughter bubbles for bubble breakage in oil as compared with that in water [14]. The correlation of number of daughter bubbles with the stirring rate in oil is given as:

$$n_d = 0007\ N^{1.17}$$

(R^2= 0.99) for 220 ≥ N≤ 430 (5)

It is evident that the dependence of the number of bubble fragments on the stirring speed in the case of the oil continuous phase is 1.17.

For the water continuous phase from the work of [14], correlation is:

$$n_d = 0.012\ N^{1.51}$$

(R^2= 0.97) for 220 ≥ N≤ 430 (6)

The dependence of the number of daughter bubbles on N for oil in Eq. (5) is lower than that of water in Eq. (6). This indicates the more effective influence of hydrodynamics in the case of water on breakage rate than in the case of oil.

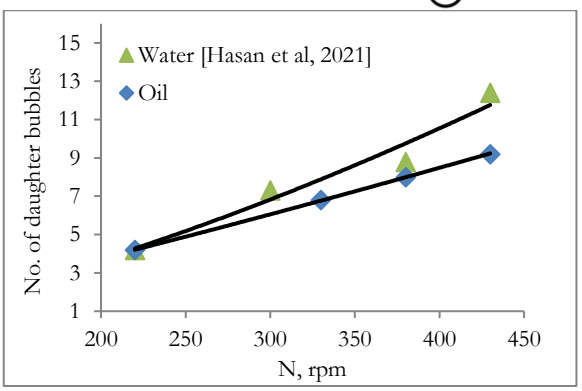

Figure 7: Average number of daughter bubbles produced in oil and water vs. N.

Similarly, from Fg.3, the breakage probability correlates with the stirring rate f l as

$$BP_{oil} = 2.1$$

(R^2= 094) for 20 ≥ N≤ 430 (7)

For water, from the data of:

$$= 5.8\ N^{0.309}$$

(R^2= 0.85) for 220 ≥ N≤ 430 (8)

It can be noted that the values of breakage probability in the case of oil are lower than that of water, but the dependence of BP on N is higher.

4. Conclusions

When injecting the bubble into a high turbulence field of oil continuous phase, it experiences different scales of deformation depending on its relative location in the tank. Different deformed shapes of bubbles in the oil continuous phase are observed such as necking, elongation, and flattening**.** The majority of bubble breakage occurs after necking deformation has occurred. The bubble breakage probability in oil is lower than in water, which indicates that the increased viscosity of a continuous phase causes a decrease in bubble breakage rate. At the highest stirring speed (430 rpm) conducted in this research, the breakage probability in both oil and water is 100% at the impeller region. In general, the multiple breakage probability in oil is slightly lower than in water. The average number of produced daughter bubbles at the highest speed (430 rpm) in the impeller region in the case of oil is 9.2 and in water is 12.4. The average number of produced daughter bubbles in the impeller region increases appreciably with agitation speed with a dependence of 1.51 in water and 1.14 in oil.

5. Acknowledgment

The authors would like to thank Alexander von Humboldt Foundation/ Germany for providing experimental tools for this work that helped to perform the experimental work. Thanks also to Dr. Richard A. Craig from the University of Adelaide for providing editorial services for this article.

6. References

[1] J. Solsvik, P. J. Becker, N. Sheibat-Othman, I. Mohallick, R. Farzad, and H. A. Jakobsen, "Viscous Drop Breakage in Liquid-Liq Stirred

Dispersions: Population Balance Modeling," *J. Dispersuid. Sci. Technol.*, vol. 36, no. 4, pp. 577–594, 2015, doi: 10.1080/01932691.2014.910471.

[2] W. Shi, J. Yang, G. Li, X. Yang, Y. Zong, and X. Cai, "Modelling of breakage rate and bubble size distribution in bubble columns accounting for bubble shape variations," *Chem. Eng. Sci.*, vol. 187, pp. 391–405, 2018.

[3] P. Chu, J. Finch, G. Bournival, S. Ata, C. Hamlett, and R. J. Pugh, "A review of bubble break-up," *Adv. Colloid Interface Sci.*, vol. 270, pp. 108–122, 2019.

[4] L. Niño, R. Gelves, H. Ali, J. Solsvik, and H. Jakobsen, "Applicability of a modified breakage and coalescence model based on the complete turbulence spectrum concept for CFD simulation of gas-liquid mass transfer in a stirred tank reactor," *Chem. Eng. Sci.*, vol. 211, p. 115272, 2020.

[5] A. Bąk and W. Podgórska, "Drop breakage and coalescence in the toluene/water dispersions with dissolved surface active polymers PVA 88% and 98%," *Chem. Eng. Res. Des.*, vol. 91, no. 11, pp. 2142–2155, 2013.

[6] K. Samaras, M. Kostoglou, T. D. Karapantsios, and P. Mavros, "Effect of adding glycerol and Tween 80 on gas holdup and bubble size distribution in an aerated stirred tank," *Colloids Surfaces A Physicochem. Eng. Asp.*, vol. 441, pp. 815–824, 2014.

[7] B. O. Hasan, "Breakage of drops and bubbles in a stirred tank: A review of experimental studies," *Chinese J. Chem. Eng.*, vol. 25, no. 6, pp. 698–711, 2017.

[8] H. Zhou, J. Yang, S. Jing, W. Lan, Q. Zheng, and S. Li, "Influence of Dispersed-Phase Viscosity on Droplet Breakup in a Continuous Pump-Mixer," *Ind. Eng. Chem. Res.*, vol. 58, no. 51, pp. 23458–23467, 2019.

[9] K. Shimizu, K. Minekawa, T. Hirose, and Y. Kawase, "Drop breakage in stirred tanks with Newtonian and non-Newtonian fluid systems," *Chem. Eng. J.*, vol. 72, no. 2, pp. 117–124, 1999.

[10] M. Nishikawa, F. Mori, and S. Fujieda, "Average drop size in a liquid-liquid phase mixing vessel," *J. Chem. Eng. Japan*, vol. 20, no. 1, pp. 82–88, 1987.

[11] M. C. Ruiz, P. Lermanda, and R. Padilla, "Drop size distribution in a batch mixer under breakage conditions," *Hydrometallurgy*, vol. 63, no. 1, pp. 65–74, 2002.

[12] M. Stamatoudis and L. L. Tavlarides, "Effect of continuous-phase viscosity on the drop sizes of liquid-liquid dispersions in agitated vessels," *Ind. Eng. Chem. Process Des. Dev.*, vol. 24, no. 4, pp. 1175–1181, 1985.

[13] C. A. Coulaloglou and L. L. Tavlarides, "Description of interaction processes in agitated liquid-liquid dispersions," *Chem. Eng. Sci.*, vol. 32, no. 11, pp. 1289–1297, 1977.

[14] B. O. Hasan, M. F. Hamad, H. S. Majdi, and M. M. Hathal, "Experimental characterization of dynamic behavior of single bubble breakage in an agitated tank," *Eur. J. Mech.*, vol. 85, pp. 430–443, 2021.

[15] H. A. Alabdly, H. S. Majdi, M. F. Hamad, M. M. Hathal, and B. O. Hasan, "Effect of impeller geometry on bubble breakage and the contributions of different breakage mechanisms in a stirred tank," *Fluid Dyn. Res.*, vol. 52, no. 6, p. 65504, 2020.

[16] R. Escudié and A. Liné, "Experimental analysis of hydrodynamics in a radially agitated tank," *AIChE J.*, vol. 49, no. 3, pp. 585–603, 2003.

[17] J. Solsvik and H. A. Jakobsen, "Single drop breakup experiments in the stirred liquid-liquid tank," *Chem. Eng. Sci.*, vol. 131, pp. 219–234, 2015, doi: 10.1016/j.ces.2015.03.059.

[18] H. J.P., *Heat Transfer*, 9th ed. New York: McGraw-Hill, 2010.

[19] S. Maaß, "Experimental analysis, modeling and simulation of drop breakage in agitated turbulent liquid/liquid-dispersions," 2011.

[20] S. F. Roudsari, G. Turcotte, R. Dhib, and F. Ein-Mozaffari, "CFD modeling of the mixing of water in oil emulsions," *Comput. Chem. Eng.*, vol. 45, pp. 124–136, 2012.

[21] R. Sanjuan-Galindo, E. Soto, R. Zenit, and G. Ascanio, "Viscous filament fragmentation in a turbulent flow inside a stirred tank," *Chem. Eng. Commun.*, vol. 202, no. 9, pp. 1251–1260, 2015.

[22] S. Kumar, V. Ganvir, C. Satyanand, R. Kumar, and K. S. Gandhi, "Alternative mechanisms of drop breakup in stirred vessels," *Chem. Eng. Sci.*, vol. 53, no. 18, pp. 3269–3280, 1998.

[23] S. Kumar, R. Kumar, and K. S. Gandhi, "Alternative mechanisms of drop breakage in stirred vessels," *Chem. Eng. Sci.*, vol. 46, no. 10, pp. 2483–2489, 1991.

[24] M. Martín, F. J. Montes, and M. A. Galán, "Influence of impeller type on the bubble breakup process in stirred tanks," *Ind. Eng. Chem. Res.*, vol. 47, no. 16, pp. 6251–6263, 2008.

[25] B. O. Hasan, "Experimental study on the bubble breakage in a stirred tank. Part 1. Mechanism and effect of operating parameters," *Int. J. Multiph. Flow*, vol. 97, pp. 94–108, 2017.

[26] V. Cristini, J. Blawzdziewicz, M. Loewenberg, and L. R. Collins, "Breakup in stochastic Stokes flows sub-Kolmogorov drops in isotropic turbulence," *J. Fluid Mech.*, vol. 492, pp. 231–250, 2003.